

## Orientational and translational disorder in semiconducting Zintl compounds

David Long Price and Marie-Louise Saboungi  
Argonne National Laboratory, Argonne, Illinois 60439

W. Spencer Howells

*Rutherford-Appleton Laboratory, Chilton, Oxon OX11 0QX, United Kingdom*  
(Received 14 November 1994; revised manuscript received 10 February 1995)

Two alkali-metal–polyvalent-metal Zintl compounds, NaSn and CsPb, exhibit a two-stage melting process with high-temperature solid phases characterized by rapid dynamical disorder. In NaSn this disorder is associated with fast reorientations of the  $\text{Sn}_4^{4-}$  polyanions closely coupled to a slower migration of the  $\text{Na}^+$  cations. In CsPb it is associated with rapid reorientations of  $\text{Pb}_4^{4-}$  polyanions with the  $\text{Cs}^+$  cations participating in the dynamical disorder on the same time scale. In both cases the disordering has dramatic effects on the electronic and ionic transport and thermodynamic properties.

### I. INTRODUCTION

Melting of a one-component solid can be thought of simply as the onset of translational disorder which breaks down the long-range order of the crystal. In a more complex system, several kinds of disorder are possible.<sup>1</sup> These can include translational disorder of one sublattice (fast-ion conductors), chemical disorder between two or more sublattices (disordered alloys), orientational disorder of molecules or complex ions (rotor phases), or lattice melting in one or two directions in the crystal (ferroelastic phases). Melting may occur in a form that all applicable disordering processes take place at one temperature—the melting point—or there can be a sequence of transitions up to the melting point where partial disordering takes place. In addition to the structural aspects of these transitions, they are often associated with dramatic changes in the macroscopic behavior, including thermodynamic, mechanical, and electrical transport properties.

The relation between atomic disorder and electrical transport in semiconductors provides a particularly interesting example of such an association. The work of Mott, Anderson, and other have shown that electron transport in amorphous semiconducting materials takes place by processes fundamentally different from those in crystalline materials.<sup>2</sup> These ideas have been extended to liquid semiconductors by Cutler<sup>3</sup> and Enderby and Barnes.<sup>4</sup> It is natural to ask how these properties evolve when the progress from ordered crystal to fully disordered liquid takes place through a sequence of transitions as described above. One example of such a sequential disordering is provided by *translational disorder* in high-temperature solid phases of materials such as  $\text{Cu}_2\text{S}$  and  $\text{Ag}_2\text{S}$ ; while their semiconducting properties have been known for some time, it is only relatively recently that it has been possible to distinguish experimentally between ionic and electronic conduction in such materials,<sup>5</sup> and even more recently that an explanation for the mutual enhancement of ionic migration and electron mobility has been put forward.<sup>6</sup>

Two semiconducting compounds have recently been identified in which *orientational as well as translational disordering* takes place in the solid prior to melting: NaSn (Ref. 7) and CsPb.<sup>8,9</sup> These are examples of Zintl phases, compounds in which electron transfer combined with directional bonding of the negative species leads to chemical behavior in these species characteristic of elements further to the right in the Periodic Table. NaSn and CsPb share with other Zintl compounds of Sn and Pb a number of unusual properties arising from the formation of tetrahedral  $\text{Sn}_4^{4-}$  or  $\text{Pb}_4^{4-}$  polyanions (“Zintl ions”). Crystal structures of these compounds have polyanions of this type arranged on a bct lattice, separated by alkali metal ions, each of which is shared by two polyanions.<sup>10</sup> In the neutron-diffraction patterns of the liquids, strong “first sharp diffraction peaks” are observed, due to dense random packing of the polyanions.<sup>11,12</sup> They are unique, as far as is known, among the Zintl compounds in exhibiting disordered solid phases prior to melting. The disordering is associated with dramatic changes in electrical transport properties.

This work presents a complete description of the dynamic disorder observed in these compounds by quasi-elastic neutron scattering (QENS). The intensity  $I(\mathbf{Q}, E)$  measured in such experiments is generally written in terms of an average scattering function  $S(\mathbf{Q}, E)$ :<sup>13</sup>

$$\begin{aligned} I(\mathbf{Q}, E) &= \frac{k_1}{k_0} \langle \bar{b}^2 \rangle S(\mathbf{Q}, E) \\ &= \frac{k_1}{k_0} \left[ \langle \bar{b}^2 \rangle S_{\text{coh}}(\mathbf{Q}, E) \right. \\ &\quad \left. + \langle \bar{b}^2 - \bar{b}^2 \rangle S_{\text{inc}}(\mathbf{Q}, E) \right], \end{aligned} \quad (1)$$

where  $\mathbf{k}_0$  and  $\mathbf{k}_1$  are the incident and scattered wave vectors,  $\bar{b}$  and  $\bar{b}^2$  are mean and mean-square neutron-scattering lengths, respectively,  $\langle \dots \rangle$  indicates an average over the elements in the sample, and  $\mathbf{Q} = \mathbf{k}_0 - \mathbf{k}_1$  and  $E = \hbar^2(k_0^2 - k_1^2)/2m_n$  are the scattering vector and ener-

gy transfer in the scattering event. On the right-hand side of Eq. (1),  $S_{\text{coh}}(\mathbf{Q}, E)$  and  $S_{\text{inc}}(\mathbf{Q}, E)$  are the coherent and incoherent scattering functions which describe the dynamics of the collective and single-particle motions, respectively.<sup>13</sup> In general, the intensity measured in a single scattering experiment will contain contributions from each of these. The total scattered intensity at scattering vector  $\mathbf{Q}$  can be written in terms of the average structure factor  $S(Q)$ :

$$S(Q) = \frac{\langle \bar{b}^2 \rangle}{\langle b^2 \rangle} [S_{\text{coh}}(Q) - 1] + 1, \quad (2)$$

where only the coherent part retains a dependence on  $\mathbf{Q}$ . In the QENS region (where  $E$  is generally small compared with the energies of the vibrational modes) for a regular crystalline phase there is always an elastic component that reflects the time-average structure, with  $S(Q, E)$  proportional to a  $\delta$  function  $\delta(E)$ .  $S_{\text{coh}}(\mathbf{Q}, E)$  is Bragg-like (nonzero only at discrete reciprocal lattice points  $\mathbf{Q}=\mathbf{h}$ ) while  $S_{\text{inc}}(\mathbf{Q}, E)$  is diffuse (nonzero at all  $\mathbf{Q}$ ). If relaxation processes are present, there is also a broadened component in  $S_{\text{coh}}(\mathbf{Q}, E)$  and  $S_{\text{inc}}(\mathbf{Q}, E)$  with the general form

$$S(\mathbf{Q}, E) = \sum_k \frac{a_k(\mathbf{Q})}{\pi} \frac{E_k(\mathbf{Q})}{E^2 + E_k(\mathbf{Q})^2}, \quad (3)$$

where  $a_k(\mathbf{Q})$  and  $E_k(\mathbf{Q})$  are the characteristic amplitude and energy of a relaxation process  $k$ ; if this process has a relaxation time  $\tau_k(\mathbf{Q})$ , then  $E_k(\mathbf{Q}) = h/\tau_k(\mathbf{Q})$ . In the case of reorientational relaxation (in rotor phases and plastic crystals) the QENS spectra have both broadened and elastic components,<sup>9,14</sup> if the reorientations are diffusive in character, the elastic component appears only in the incoherent part.<sup>15</sup> In the case of translational relaxation (in fast-ion phases), only the broadened components occur in the scattering from the migrating species.<sup>16</sup> In fluid phases there is no time-average structure and all the scattering is broadened.

Section II contains results from NaSn, giving experimental details beyond those provided in an earlier work<sup>7</sup> and presenting new data which provide evidence that a second time scale is involved. Results on the liquid phase are also presented, since the interpretation of these data corroborates that of the disordered solid phase. Section III provides a brief summary of results previously published<sup>8</sup> on the disordered solid phase of CsPb, for the purpose of comparing the behavior of the two compounds. In addition, QENS data in the liquid phase are presented for the first time. Finally, Sec. IV summarizes and contrasts the dynamic disorder of CsPb and NaSn and relates their atomic disorder to the observed electrical transport properties.

## II. SODIUM-TIN

Na-Sn is observed to have a complex melting behavior, exhibited in the calorimetric data<sup>17</sup> shown in Fig. 1. The existence of two solid phases was first established by Hume-Rothery,<sup>18</sup> who did not however speculate about their nature. The crystal structure at low temperature<sup>19</sup>

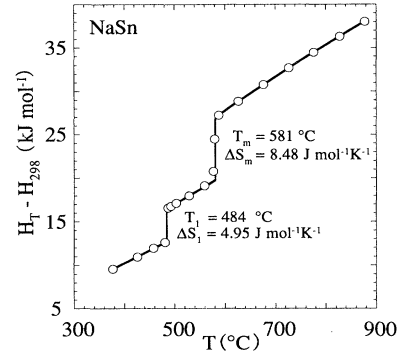


FIG. 1. Enthalpy of NaSn as a function of temperature (Ref. 17).

is the same as in CsPb and the other Zintl compounds of Sn and Pb with the alkali metals (except Li). To investigate the possibility of dynamic disorder in the high-temperature solid phase, QENS measurements were carried out in the two solid phases and in the liquid at the IRIS and HET spectrometers at ISIS. Numerical values of relevant neutron scattering parameters for NaSn and CsPb are given in Table I.

IRIS is a time-of-flight backscattering spectrometer in which the energy-transfer window is defined by the range of wavelengths in the neutron pulse and the scattered neutron energy is set with an array of either pyrolytic graphite or mica analyzers.<sup>20</sup> In this experiment only the graphite analyzer array was used, with the option of two reflections. With the [002] reflection a  $Q$  range up to  $2 \text{ \AA}^{-1}$  was accessible with an energy-transfer range of about  $\pm 0.5 \text{ meV}$  and energy resolution about  $15 \text{ } \mu\text{eV}$ , while with the [004] reflection the  $Q$  range doubled to give a maximum value of about  $4 \text{ \AA}^{-1}$  with an energy-transfer range of several meV and energy resolution about  $50 \text{ } \mu\text{eV}$ . In this experiment the [002] reflection gave more useful results and the data presented were taken in this configuration. In addition to the energy analyzer-detector system, IRIS has a diffraction detector at high angle which is invaluable for measuring the total scattering and monitoring the phase of the sample. The latter was contained in a sealed Zircaloy cylindrical container of inner diameter 9.5 mm and wall thickness 0.6 mm, mounted vertically in a vacuum furnace with niobium resistance heating element and radiation shields; niobium was used to minimize the incoherent elastic scattering. The data were analyzed using routines from the IRIS Data Analysis (IDA) program package.<sup>21</sup> The raw data were converted into  $S(Q, E)$  form [Eq. (1)],

TABLE I. Values of scattering lengths for CsPb and NaSn. [V. F. Sears, in *Neutron Scattering* (Ref. 13), Part A, p. 521.]

AM	CsPb	NaSn
$\bar{b}_A$ (fm)	5.42	3.63
$\bar{b}_M$ (fm)	9.405	6.226
$\langle \bar{b}^2 - \bar{b}^2 \rangle_A$ (fm <sup>2</sup> )	1.67	12.89
$\langle \bar{b}^2 - \bar{b}^2 \rangle_M$ (fm <sup>2</sup> )	0.02	0.18
$\langle \bar{b}^2 \rangle$ (fm <sup>2</sup> )	59.76	32.52

corrected for container scattering and sample absorption, and normalized to a standard vanadium sample. The widths of the quasielastic peaks were determined using two methods: a least-squares-fitting procedure involving the convolution of sample scattering with the measured resolution function, and an analysis using Bayesian statistics;<sup>22</sup> the results shown here correspond to the latter option.

HET is a time-of-flight inelastic chopper spectrometer using direct geometry and viewing the ambient temperature moderator.<sup>20</sup> The detector angle range used was  $3^\circ$ – $29^\circ$  and the incident energy was set by a multislit chopper with an energy resolution of about 2%. In this experiment two incident energies, 20 and 40 meV, were used. With an energy of 20 meV, a  $Q$  range up to about  $1.5 \text{ \AA}^{-1}$  was accessible with an energy resolution of about 0.4 meV, while with an energy of 40 meV the  $Q$  range increased to about  $2.2 \text{ \AA}^{-1}$  with an energy resolution of 0.8 meV. The sample was contained in three Zircaloy tubes of the same type used on IRIS, mounted vertically above each other with axes horizontal. They were heated in a vacuum furnace of the same type used on IRIS but with a horizontal axis. The data were reduced to  $S(Q, E)$  using the HOMER program<sup>23</sup> and the quasielastic peaks fitted using a program from the IDA package. The low-temperature solid phase was used to provide the resolution function, and data at  $Q$  values around the Bragg peaks from the sample were omitted.

### A. Disordered solid

QENS spectra measured on the IRIS spectrometer are shown in Fig. 2 and exhibit characteristic broadening in both the  $\alpha$  solid and liquid phases. Especially remarkable, in view of the significant incoherent scattering cross section of Na, is the absence of observable diffuse elastic scattering in the  $\alpha$  phase, which is zero within experimental error when averaged over all angles except those corresponding to  $Q$  values near  $1 \text{ \AA}^{-1}$  where there is considerable Bragg scattering. For reasons discussed in Sec. I, the absence of significant incoherent elastic scattering indicates that the dynamic disorder associated with the  $\text{Na}^+$  ions is translational, rather than orientational, in nature.

The intensities of the single Lorentzian functions fitted to the spectra measured on IRIS and HET at each angle are shown as a function of  $Q$  in Fig. 3, and the widths are shown in Fig. 4. The HET results show a broad component whose width and intensity both increase considerably at higher  $Q$ . This component is not seen in the IRIS data at higher  $Q$  because it is too broad to show up within the IRIS window ( $\pm 0.4$  meV). On the other hand, the IRIS data show a much narrower component whose intensity falls rapidly with  $Q$  which is too narrow to be picked out on top of the broad component in the poorer resolution HET data. The summed intensity of the two components agrees with the total scattering measured in the diffraction detector and hence accounts for all the diffuse scattering. In Fig. 4, the measured widths of the IRIS data are seen to be in reasonable agreement with a Chudley-Elliott jump diffusion model<sup>24</sup>

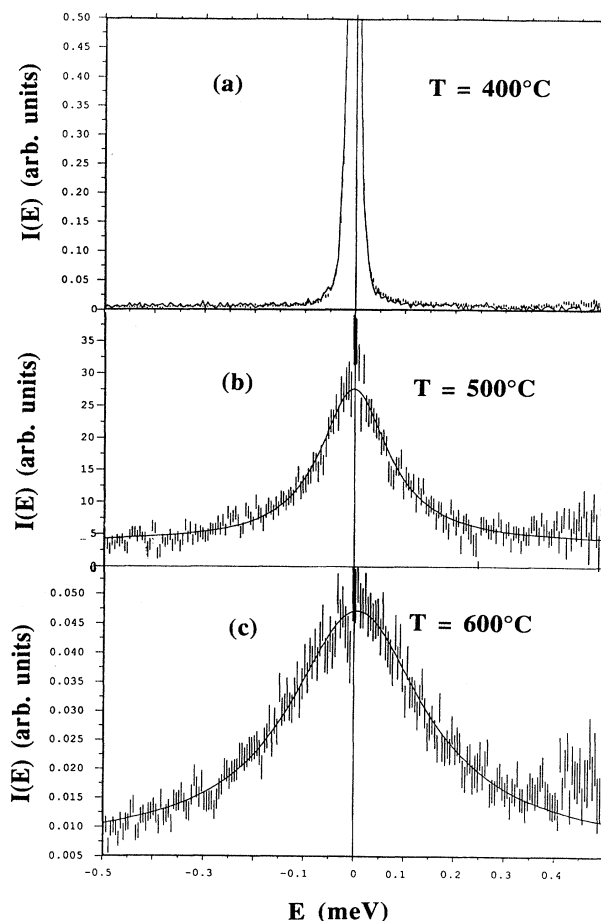


FIG. 2. QENS spectra from NaSn for  $52.4^\circ$  scattering angle at three temperatures corresponding to the  $\beta$ ,  $\alpha$ , and liquid phases: data (bars) and fitted resolution-broadened  $\delta$  function in (a) and Lorentzian functions in (b) and (c) (lines).

$$E_k = \frac{\hbar}{\tau} \sum_l [1 - \exp\{i\mathbf{Q}\cdot\mathbf{l}\}] \quad (4)$$

with two parameters, a jump distance  $l$  of  $3.75 \text{ \AA}$  (similar to the shortest Na-Na distances in the  $\beta$  crystal) and a jump time  $\tau$  of 7.3 ps, represented by the solid curve. It

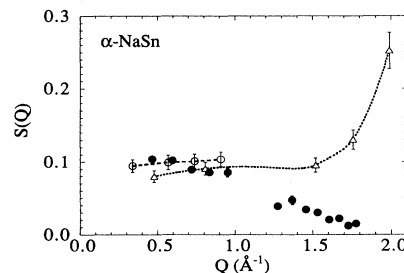


FIG. 3. Intensities of fitted Lorentzian peaks for  $\alpha$ -NaSn at  $500^\circ\text{C}$ :  $\bullet$ , IRIS;  $\circ$ , HET (20 meV);  $\triangle$ , HET (40 meV). Values near  $Q = 1 \text{ \AA}^{-1}$  are omitted because the spectra contain considerable Bragg scattering. The lines joining the points are a guide to the eye only.

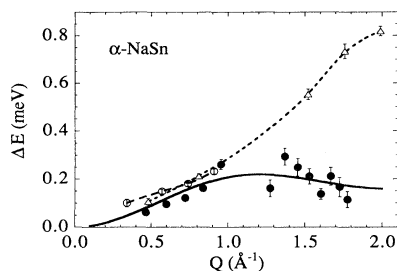


FIG. 4. Measured full width at half maximum of the fitted resolution-broadened Lorentzian peaks for  $\alpha$ -NaSn at 500°C: ●, IRIS; ○, HET (20 meV); △, HET (40 meV); the solid curve is calculated from a simple jump-diffusion model. The dotted and dashed lines joining the points are a guide to the eye only.

is therefore reasonable to associate this narrow component with the  $\text{Na}^+$  migration and in the broad component with the more rapid reorientations of the  $\text{Sn}_4^{4-}$  polyanions. The absence of significant elastic diffuse scattering indicates that these reorientations are diffusive in nature, as discussed in Sec. I.

Taken together, these results show that the  $\alpha$  phase of NaSn is dynamically disordered. The dynamic disorder consists of rapid reorientations of the polyanions (fast rotor behavior) which enhance the slower cation migration (fast-ion conduction): this situation is schematically illustrated in Fig. 5. Although the jump frequencies are different, the two processes must be strongly coupled since only one phase transition is observed prior to melting. The paddle-wheel migration of the  $\text{Na}^+$  resembles that of  $\text{Li}^+$  in  $\alpha$ - $\text{LiSO}_4$  and analogous sulfates.<sup>25</sup> More recently, coupled rotational and translational disorder has been observed in  $\text{AC}_{60}$  alloys.<sup>26</sup> A related phenomenon is proton diffusion in hydrogen-bonded crystals by means of a Grotthus mechanism involving alternating rotational and translational jumps;<sup>27</sup> however, this situation differs from the present case in that each mobile ion site can be associated with a single center.

Electrical transport in NaSn is coupled to the dynamic atomic disorder. Recent results for the electrical conductivity<sup>28</sup> show a *drop* in conductivity at the  $\beta$ - $\alpha$  transition, presumably reflecting the additional scattering associated with the dynamic disorder; in contrast, any ionic component of the measured conductivity must *increase* at the transition. The large jump within the  $\alpha$  phase reflects a close coupling between atomic migration and electronic mobility, discussed in depth by Fortner *et al.*<sup>28</sup> There appears to be little if any change in the conductivity on melting. NaSn appears to transform to a crystallographic phase of lower symmetry, apparently orthorhombic,<sup>29</sup> at the disordering transition, an unusual example of lattice symmetry lowering at such a transition.

### B. Liquid

As illustrated in the example in Fig. 2, the quasielastic scattering spectra in the liquid have a general resemblance to those of the disordered solid but with larger widths. The intensities of the Lorentzian functions fitted to the IRIS and HET data are shown as a function of  $Q$

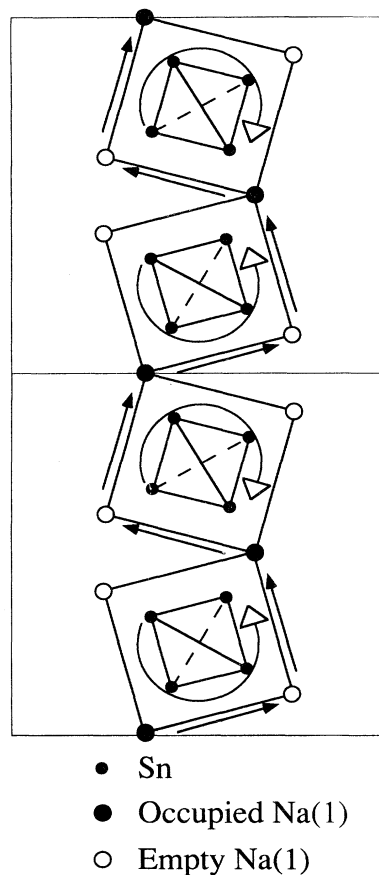


FIG. 5. Schematic illustration of migration in  $\alpha$ -NaSn.

in Fig. 6, and the widths in Fig. 7. Again, the HET data show a broad component, and the IRIS data a narrow component, at higher  $Q$ . The peak in the intensity and the dip in the width (due to de Gennes narrowing) of the narrow component around  $Q \approx 1 \text{ \AA}^{-1}$  reflect the first sharp diffraction peak that is observed in the total scattering in this region, although this feature is not as strong as in the heavier alkali-metal compounds. As in the  $\alpha$  phase, it is reasonable to associate the narrow component with the center-of-mass motions, now including those of the  $\text{Sn}_4^{4-}$  polyanions as well as the  $\text{Na}^+$  ions, and a broad component with the more rapid polyanion reorientations.

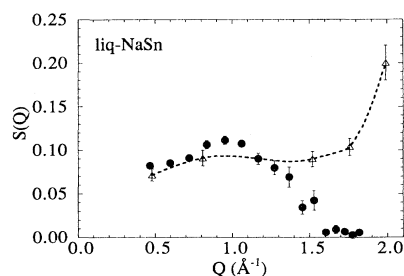


FIG. 6. Intensities of fitted Lorentzian peaks for liquid NaSn at 600°C: ● IRIS; △, HET (40 meV). The lines joining the points are a guide to the eye only.

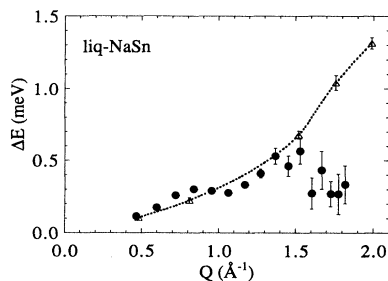


FIG. 7. Measured full width at half maximum of the fitted resolution-broadened Lorentzian peaks for liquid NaSn at 600 °C: ●, IRIS; △, HET (40 meV). The lines joining the points are a guide to the eye only.

### III. CESIUM-LEAD

The enthalpy functions of CsPb and KPb were measured by Johnson and Saboungi.<sup>30</sup> Whereas KPb has a single melting transition, CsPb has two transitions about 50 K apart, with the enthalpy and entropy of melting split rather evenly between them. While the behavior of the enthalpy function resembles NaSn, the behavior of Cp is quite different in the two compounds.<sup>17,30</sup> The structure of the three phases of CsPb was established in neutron-diffraction measurements.<sup>9</sup> The structure factors of the low-temperature ( $\beta$ ) crystalline phase and the liquid were similar to those of other Sn (Ref. 11) and Pb (Ref. 12) Zintl compounds, while that of the intermediate ( $\alpha$ ) phase combined a feature at  $Q \sim 1 \text{ \AA}^{-1}$  that appeared to be a set of unresolved Bragg peaks with a diffuse, non-crystalline pattern at larger  $Q$ .

#### A. Disordered solid

The overall picture suggested by the diffraction data, a crystalline phase with extensive disorder, was confirmed by inelastic neutron-scattering measurements carried out on the IN-6 spectrometer at ILL.<sup>8,9</sup> It is useful to summarize the results here in order to compare with NaSn. In the  $\beta$  phase the QENS spectra have the shape of the unbroadened resolution function of the instrument. In the  $\alpha$  phase they show a superposition of unbroadened and broadened components that can be well represented by a  $\delta$  function and single Lorentzian function, respectively, both broadened by the resolution function. The  $\delta$  function intensity peaks in the region of the Bragg peaks at  $Q \sim 1 \text{ \AA}^{-1}$ , but has a significant, nonzero value over the rest of the measured  $Q$  range, while the Lorentzian-function intensity has a low maximum just to the left of the Bragg peaks ( $Q \sim 0.9 \text{ \AA}^{-1}$ ) and then starts to rise to large values at  $Q \sim 1.5 \text{ \AA}^{-1}$ ; the dramatic rise in intensity above  $1.5 \text{ \AA}^{-1}$  is reminiscent of that found in NaSn (Fig. 3). The sum of the two appears to account for the static structure factor measured in the diffraction experiment.<sup>9</sup>

To extract quantitative information, a simple model was adopted in which  $\text{Cs}_4\text{Pb}_4$  units were assumed to undergo independent, random jumps between the four orientations found in the  $\beta$  crystal structure in succession as one moves up the  $c$  axis.<sup>9</sup> Since these orientations are unequally spaced, two jump times,  $\tau_1$  and  $\tau_2$ , were as-

sumed for nearest- and next-nearest-neighbor jumps, respectively. The quasielastic scattering spectra calculated from this model showed both unbroadened and broadened components similar to the measured ones. The integrated intensities of the two components, which are independent of the values of  $\tau_1$  and  $\tau_2$ , are in excellent agreement with the measured values averaged over the different runs (see Fig. 10 of Ref. 9). The widths of the broadened spectra do not agree so well and are relatively insensitive to the ratio  $\tau_1/\tau_2$  (see Fig. 11 of Ref. 9). Other problems with the simple model are (a) that it predicts too low a value for the entropy change at the  $\beta$ - $\alpha$  transition,  $0.5 \ln 2$  per formula unit compared with the measured value<sup>30</sup> of  $7.15 \text{ J mol}^{-1} \text{ K}^{-1}$  which is nearly five times higher, (b) that it neglects correlations between the different Zintl ions which are clearly required to produce a phase transition, and (c) that it overlooks the fact that  $\text{Cs}^+$  ions in the  $\beta$ -phase crystal are each shared by two  $\text{Pb}_4^{4-}$  polyanions and presumably are in the  $\alpha$  phase as well. Nevertheless, models in which only  $\text{Pb}_4^{4-}$  polyanions reorient independently do not reproduce the first peak in the intensity of the Lorentzian component at  $Q \approx 0.9 \text{ \AA}^{-1}$ . The  $\text{Cs}^+$  cations must therefore be participating in some way in the dynamic disorder, apparently on a similar time scale to that of the  $\text{Pb}_4^{4-}$  reorientations since only one linewidth is observed in the QENS spectra of the  $\alpha$  phase. This behavior contrasts with that of NaSn where, as discussed in Sec. II A, the polyanion rotations and cation motions appear to take place on different time scales.

The dc electrical conductivity of CsPb rises sharply at the  $\beta$ - $\alpha$  transition, indicating a significant decrease in the gap in  $\sigma(E)$ .<sup>28</sup> It increases slowly with temperature in the  $\alpha$  phase, and drops slightly at the melting point. This behavior is also quite different from NaSn where the large increase in conductivity takes place within the  $\alpha$  phase. Analysis of the Bragg peaks around  $Q = 1 \text{ \AA}^{-1}$  suggests that the structure of the disordered phase of NaSn is also of lower symmetry than that of the ordered phase; in this case the unit cell appears to be triclinic.<sup>29</sup>

#### B. Liquid

Analysis of the QENS spectra in the liquid phase shows that two Lorentzian functions are necessary to fit the data. The  $Q$  variation of the intensities of the two components up to  $Q = 1.65 \text{ \AA}^{-1}$  is shown in Fig. 8 and

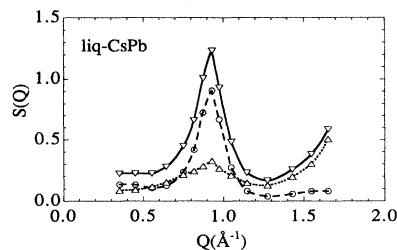


FIG. 8. Measured intensities of narrow (○) and broad (△) Lorentzian peaks and total intensities (▽) for liquid CsPb at 923 K. The lines joining the points are a guide to the eye only.

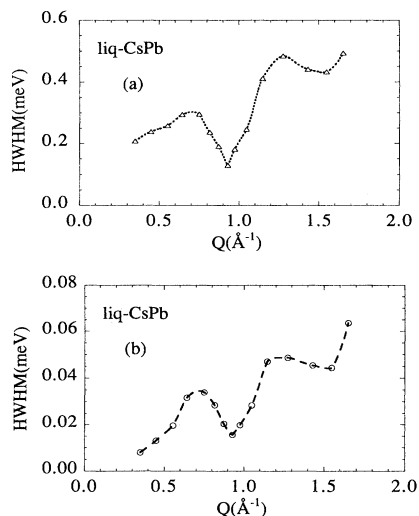


FIG. 9. Measured halfwidths at half maximum (circles) of (a) broad and (b) narrow Lorentzian peaks for liquid CsPb at 923 K. The lines joining the points are a guide to the eye only.

that of their widths (half width at half maximum) in Fig. 9. The  $Q$  variation of the intensities is quite different for the two components but remarkably similar to that of the Lorentzian and  $\delta$ -function components in the  $\alpha$  phase.<sup>9</sup> The widths of the two components differ by about a factor 8 but have a qualitatively similar behavior; they have also some qualitative resemblance to the widths of the broadened component in the  $\alpha$  phase, but the variations are more pronounced; the dips near  $Q \approx 0.9 \text{ \AA}^{-1}$  reflects de Gennes narrowing arising from the peak in  $S(Q)$ .<sup>12</sup>

Comparison of the results for the  $\alpha$  and liquid phases indicates that the elastic component in the  $\alpha$  phase is broadened to become the narrow Lorentzian component in the liquid. It is reasonable to associate this component with diffusion of the centers of mass of the  $\text{Pb}_4^{4-}$  polyanions, which from the diffraction experiments appear to be stable in the liquid.<sup>12</sup> The broad component can then be identified with rotational diffusion of these units and associated motions of the  $\text{Cs}^+$  cations on a similar time scale, since the intensity shows a peak at  $Q \approx 0.9 \text{ \AA}^{-1}$  as in the  $\alpha$  phase. This again contrasts with liquid NaSn where the cation motions and polyanion rotations appear to take place on different time scales. The widths of the broad component are, within experimental accuracy, consistent with an inelastic neutron scattering measurement<sup>12</sup> on KPb made with an incident energy of 50 meV, thus covering a much larger  $Q$  range but at lower resolution. In that measurement the width could be fitted over the entire range by a simple diffusion ex-

pression

$$E_k = \hbar D Q^2 \quad (5)$$

[equivalent to Eq. (4) with large  $l$  and  $D = l^2/3\tau$ ] with  $D = 1.2 \pm 0.2 \times 10^{-5} \text{ cm}^2 \text{ s}^{-1}$ , a value somewhat lower than that found in pure liquid lead,  $2.2 \times 10^{-5}$ , and thus consistent with the picture of diffusing polyanions.

#### IV. CONCLUSIONS

Two alkali-metal–polyvalent-metal Zintl compounds, NaSn and CsPb, exhibit a two-stage melting process with high-temperature ( $\alpha$ ) solid phases characterized by rapid dynamical disorder. In NaSn this disorder is associated with fast reorientations of the  $\text{Sn}_4^{4-}$  polyanions closely coupled to a slower migration of the  $\text{Na}^+$  cations. In CsPb it is associated with rapid reorientations of  $\text{Pb}_4^{4-}$  polyanions with the  $\text{Cs}^+$  cations participating in the dynamical disorder on the same time scale. Preliminary measurements of NMR relaxation rates and line shapes in both compounds appear to confirm these conclusions.<sup>31</sup> The two compounds provide novel examples of translation-rotation coupling in orientationally disordered crystals, discussed in the review of Lynden-Bell and Michel.<sup>32</sup> The liquid phases in both compounds exhibit dynamic effects on two distinct time scales reflecting the relatively slow center-of-mass motions of the polyanions and the relatively fast polyanion rotations; the cation motions are on the time scale of the center-of-mass motions in NaSn and on that of the reorientations in CsPb. The  $\alpha$  phases of both NaSn and CsPb are characterized by a lower crystalline symmetry than the low-temperature ( $\beta$ ) phases. Significant distortions are apparently required to accommodate the additional partly filled cation sites that are needed for the dynamical disorder and which make the disordered phase entropically favorable. The detailed atomic arrangements in these structures are the subject of a diffraction study in progress.

#### ACKNOWLEDGMENTS

The authors are grateful to M. Conradi, J. E. Enderby, and W. van der Lugt for many illuminating discussions, M. Adams and T. Perrin for helpful guidance with the IRIS and HET experiments on NaSn, R. Kleb for the design, and C. Konicek for the electron-beam welding, of the Zircaloy containers. They also acknowledge the invaluable support of the operations staffs at IPNS, ILL, and ISIS. This work was supported by the U.S. Department of Energy, Materials Sciences, Basic Energy Sciences, under Contract No. W-31-109-ENG-38.

<sup>1</sup>A. R. Ubbelohde, *The Molten State of Matter: Melting and Crystal Structure* (Wiley, Chichester, 1978).

<sup>2</sup>N. F. Mott, *Conduction in Non-Crystalline Materials*, 2nd. ed. (Clarendon, Oxford, 1993); *Metal-Insulator Transitions*, 2nd. ed. (Taylor & Francis, London, 1991).

<sup>3</sup>M. Cutler, *Liquid Semiconductors* (Academic, New York,

1977).

<sup>4</sup>J. E. Enderby and A. C. Barnes, *Rep. Prog. Phys.* **53**, 85 (1990).

<sup>5</sup>C. Wagner, *Z. Phys. Chem.* **21**, 42 (1933).

<sup>6</sup>S. Ramasesha, *J. Solid State Chem.* **41**, 333 (1982).

<sup>7</sup>M.-L. Saboungi, J. Fortner, W. S. Howells, and D. L. Price, *Nature* **365**, 237 (1993).

- <sup>8</sup>D. L. Price, M.-L. Saboungi, H. T. J. Reijers, G. Kearley, and R. White, *Phys. Rev. Lett.* **66**, 1894 (1991).
- <sup>9</sup>D. L. Price and M.-L. Saboungi, *Phys. Rev. B* **44**, 7289 (1991).
- <sup>10</sup>R. E. Marsh and D. P. Shoemaker, *Acta Crystallogr.* **6**, 197 (1953).
- <sup>11</sup>B. P. Alblas, W. van der Lugt, J. Dijkstra, W. Geertsma, and C. van Dijk, *J. Phys. F* **13**, 2465 (1983); H. T. J. Reijers, M.-L. Saboungi, D. L. Price, and W. van der Lugt, *Phys. Rev. B* **41**, 5661 (1990).
- <sup>12</sup>H. T. J. Reijers, M.-L. Saboungi, D. L. Price, J. W. Richardson, K. J. Volin, and W. van der Lugt, *Phys. Rev. B* **40**, 6018 (1989).
- <sup>13</sup>D. L. Price and K. Sköld, in *Neutron Scattering*, edited by E. Sköld and D. L. Price (Academic, San Diego, 1986), Part A, p. 1.
- <sup>14</sup>M. Bée, *Quasielastic Neutron Scattering* (Hilger, Bristol, 1988).
- <sup>15</sup>D. A. Neumann, J. R. D. Copley, R. L. Cappelletti, W. A. Kamitakahara, R. M. Lindstrom, K. M. Creegan, D. M. Cox, W. J. Romanow, N. Coustel, J. P. McCaulay, Jr., N. C. Maliszewsky, J. E. Fischer, and A. B. Smith, III, *Phys. Rev. Lett.* **67**, 3808 (1991).
- <sup>16</sup>N. H. Anderson, K. N. Clausen, and J. K. Kjems, in *Neutron Scattering* (Ref. 13), Part B, p. 187.
- <sup>17</sup>M.-L. Saboungi, G. K. Johnson, and D. L. Price, in *Statics and Dynamics of Alloy Phase Transformations*, edited by P. E. A. Turchi and A. Gonis (Plenum, New York, 1994), p. 195.
- <sup>18</sup>W. Hume-Rothery, *J. Chem. Soc.* **131**, 947 (1928).
- <sup>19</sup>W. Müller and K. Volk, *Z. Naturforsch. B* **32**, 709 (1977).
- <sup>20</sup>B. C. Boland, Rutherford-Appleton Laboratory Report No. RAL-90-041, 1990.
- <sup>21</sup>W. S. Howells (unpublished).
- <sup>22</sup>D. S. Sivia, C. J. Carlile, W. S. Howells, and S. König, *Physica B* **182**, 341 (1992).
- <sup>23</sup>R. Osborn (private communication).
- <sup>24</sup>C. T. Chudley and R. J. Elliott, *Proc. Phys. Soc.* **77**, 353 (1961).
- <sup>25</sup>A. Lünden, *Solid State Ion.* **68**, 77 (1994), and references therein.
- <sup>26</sup>Q. Zhu, O. Zhou, J. E. Fischer, A. R. McGhie, W. J. Romanow, R. M. Strongin, M. A. Cichy, and A. B. Smith, III, *Phys. Rev. B* **47**, 13 948 (1993).
- <sup>27</sup>R. E. Lechner, Th. Dippel, R. Marx, and I. Lamprecht, *Solid State Ion.* **61**, 47 (1993).
- <sup>28</sup>J. Fortner, M.-L. Saboungi, and J. E. Enderby, *Phys. Rev. Lett.* **74**, 1415 (1995).
- <sup>29</sup>J. W. Richardson, D. L. Price, and M.-L. Saboungi (private communication).
- <sup>30</sup>G. K. Johnson and M.-L. Saboungi, *J. Chem. Phys.* **86**, 6376 (1987); M.-L. Saboungi, H. T. J. Reijers, M. Blander, and G. K. Johnson, *ibid.* **89**, 5869 (1988).
- <sup>31</sup>R. D. Stoddard, M. S. Conradi, and A. F. McDowell (private communication).
- <sup>32</sup>R. M. Lynden-Bell and K. H. Michel, *Rev. Mod. Phys.* **66**, 721 (1994).